PARALLEL TEMPERING MONTE CARLO SIMULATIONS OF $(H_2O)_6^-$

by

Suzanne Denise Gardner

B.S., Chemistry, Juniata College, 2004

Submitted to the Graduate Faculty of

Arts and Sciences in partial fulfillment

of the requirements for the degree of

Master of Science

University of Pittsburgh

2006

UNIVERSITY OF PITTSBURGH

FACULTY OF ARTS AND SCIENCES

This thesis was presented

by

Suzanne Denise Gardner

It was defended on

July 21, 2006

and approved by

Hrvoje Petek, Professor, Department of Physics and Chemistry

Peter E. Siska, Professor, Department of Chemistry

Thesis Advisor: Kenneth D. Jordan, Professor, Department of Chemistry

PARALLEL TEMPERING MONTE CARLO SIMULATIONS OF $(H_2O)_6^-$

Suzanne Denise Gardner, M.S.

University of Pittsburgh, 2006

We present a new model for characterizing the interactions of excess electrons with $(H_2O)_n^-$ clusters. This model combines a modified Thole-type water model with distributed point polarizable, denoted DPP, with quantum Drude oscillators for treating polarization and dispersion interactions between the excess electron and the water molecules. It is demonstrated by examining several small water clusters that this model closely reproduces the relative energies of different isomers of the anions as well as the electron binding energies from *ab initio* MP2 calculations. The Drude/DPP model is used to carry out parallel tempering Monte Carlo simulations of $(H_2O)_6^-$.

TABLE OF CONTENTS

LIST OF TABLES

LIST OF FIGURES

PREFACE

I wish to thank my Thesis Committee, Profs. Ken Jordan, Hrvoje Petek, and Peter Siska for their insight while preparing this thesis. I would also like to thank Thomas Sommerfeld, Albert DeFusco, and Kadir Diri for their help with this project. This work was funded by NSF and the Department of Energy. CPU time was provided by the Center for Molecular and Materials Simulations at the University of Pittsburgh.

1.0 INTRODUCTION

The chemistry of excess electrons interacting with water clusters is relevant to many fields of science, including radiation chemistry, biology, atmospheric chemistry, and medicinal chemistry. Radiation chemistry processes encompass aspects of nuclear chemistry where ionizing radiation leads to infrastructure corrosion. Photosynthesis involves long-distance electron transfer, and the interaction of excess electrons with macromolecules, such as DNA, is important because electrons have the ability to break bonds and to cause significant damage in biologically important molecules.[1] In both cases, the big biomolecules are in the presence of water, and a complete understanding of the process involved requires understanding the interactions of excess electrons with water.

Because water plays an important role in many scientific processes, understanding its fundamental chemistry is beneficial for all areas of science. To understand water interactions on a fundamental level, theoretical chemistry is utilized to simulate aqueous systems. These interactions can be water molecules interacting with each other or with another species. In the case of this research, we study water clusters interacting with excess electrons.

2.0 HISTORY OF EXCESS ELECTRON AND WATER CLUSTERS

The nature of an excess electron bound to water clusters has attracted considerable attention recently, with the 2005 publications of the Head-Gordon, Neumark, Rossky, and Johnson groups.[2,3,4,5] These studies include experimental and theoretical investigations into the properties of anionic water clusters. Simulations that use model potentials are helpful in determining the isomers that are found experimentally. Several models have been used to describe polarization, dispersion effects, and electrostatics in an attempt to match experimental data.[6,7,8,9,10,11] These models will ultimately help to answer the question of whether the excess electron is interior or surface-bound to the water cluster.[12] This thesis will review the various water cluster models that are implemented for excess electron interactions and will present a new model for describing excess electrons interactions with water.

In this work, I focus on the $(H_2O)_6^-$ cluster. $(H_2O)_6^-$ is an interesting cluster because it exhibits a well-defined vibrational spectrum in the OH stretch region.[13] Although several structures have been suggested for $(H_2O)_6^-$, a definitive assignment for the spectrum was made only recently. In 2004, Johnson and coworkers designed an experiment to determine the neutral structure of $(H_2O)_6$ that leads to the observed anion. This was done by monitoring the formation of $(H_2O)_6^-$ with IR absorption by $(H_2O)_6Ar_{10\text{-}12}$ and electron capture. The best agreement between the measured spectrum and that calculated theoretically for various isomers led to the conclusion that the precursor has a book-like structure. Although this work established the structure of the observed $(H_2O)_6^-$ anion and its neutral precursor, important questions remained.

In the present work, I use model potential approaches to characterize $(H_2O)_6^-$ at finite temperatures and to elucidate the structure of the low lying isomers. These calculations show that the low-energy isomer for $(H_2O)_6^-$ is the non-double-acceptor (non-AA) cage isomer. This differs from experimental data, which shows that the dominant isomer observed experimentally was an open-prism double acceptor (OP2-AA) structure.[14]

3.0 METHODOLOGY

3.1 ELECTRON-WATER MODELS

In describing an excess electron interacting with a water cluster, we need to take into account the electron-water interactions as well as the water-water interactions. To describe the electron-water interactions, early models allowed for electrostatic interactions and the polarization of water molecules by the excess electron. However, these models did not include dispersion interactions that make a large contribution to the electron binding energy (EBE), the energy needed to bind an electron to the water cluster by,

$$E_{anion} = E_{neutral} + E_{EBE} \qquad (1)$$

where the energy of the anion is equal to the sum of the energy of the neutral cluster and the EBE. The EBEs provide an important measure of the success of the underlying water model. If the EBEs are accurately described it means that the electrostatics, polarization and dispersion interactions are being treated correctly.

Electron correlation effects were included in recent *ab initio* studies of $(H_2O)_n^-$ ions by the Head-Gordon group.[15,16] Their work showed that the electron correlation for excess electron

systems is important for both interior and surface-bound anions. However, the Møller-Plesset perturbation theory (MP2) calculations that they used are computationally demanding, and large clusters cannot be investigated by these *ab initio* means.

In 2002, Wang and Jordan presented a new model for describing excess electron and water interactions through the use of Drude oscillators[17]. Each Drude oscillator consists of charges q+ and q-, coupled harmonically through the force constant *k* and separated by a distance R (*Figure 3.1).* The Drude model is a one-electron model potential used to calculate the binding energies of excess electrons interacting with water. Unlike conventional one-electron models, the Drude model is able to account for electron-water monomer polarization and dispersion interactions. This procedure allows the user to reduce CPU time compared to *ab initio* CCSD(T) calculations while still achieving similar binding energies.

The model Hamiltonian for an excess electron interacting with a single water molecule is

$$H = H_{el} + H_{osc} + V_{eD} \qquad (2)$$

where the individual terms are the electronic Hamiltonian, the oscillator Hamiltonian, and the coupling between the electron and Drude oscillator. The coupling term is of the form

$$V_{eD} = \frac{qr \bullet R}{r^3} f(r) \qquad (3)$$

where r is the position vector of the electron relative to the center of the Drude oscillator and R is the vector of the position of the +q charge of the Drude oscillator relative to –q, which is fixed. $f(r)$ is a damping factor, used to cut off short-range interactions. The choice of the damping factor is important, since an inaccurate damping factor will incorrectly describe short-range interactions.

In the work of Wang and Jordan, the Drude model is combined with the Dang-Chang

(DC) model[18], and an oscillator would be placed on each monomer at the position of the M site (*Figure 3.2)*.

In order to calculate the polarization and dispersion interactions, the Drude oscillator and the excess electron are treated quantum mechanically. The EBE is calculated using three levels of theory:

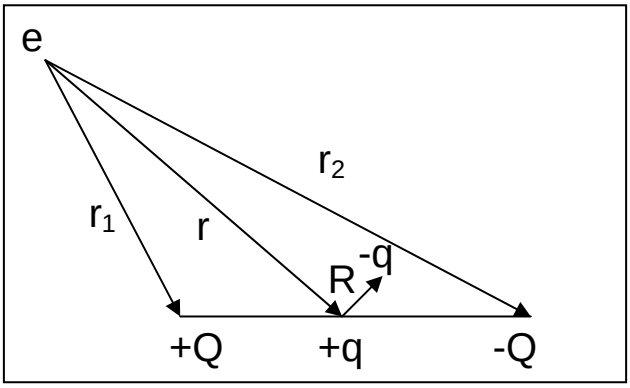

Figure 3.1 Drude model for describing an excess electron interacting with a neutral molecule with a permanent dipole moment. The dipole moment is described by the charges, +Q and –Q, which are separated by a distance $|r_1-r_2|$. The fixed charge +q is the fictitious oscillator charge. The –q charge is associated with the Drude oscillator sepated from the charge +q by the distance R.

electrostatics, second-order perturbation theory and configuration interaction (CI) methods. The Hamiltonian for an excess electron interacting with a water monomer (neglecting polarization and dispersion) is taken to be,

$$H_{el} = -\frac{1}{2}\nabla^2 - \sum_j \frac{Q_j}{r_j} + V^{ex} + V^{rep} \qquad (4)$$

where the sum is over the charge sites of the monomer and V^{rep} and V^{ex} are the short-range repulsions and exchange interactions between electron-molecule, respectively. Eq. (4) is also referred to as the electronic Hamiltonian. V^{rep} is used in accordance with Schnitker and Rossky's[19] procedure, except we present it in terms of Gaussian, not Slater functions.[20] They determined V^{rep} by imposing orthogonality between the orbital occupied by the excess electron and the filled orbitals of the neutral monomer. According to Schnitker and Rossky, V^{ex} is ignored because it is expected to contribute minimally for electron binding energy of water clusters. The oscillator Hamilitonian is

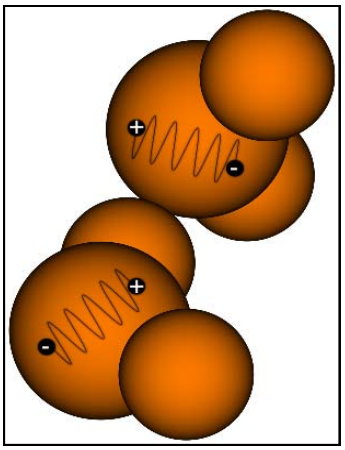

Figure 3.2 Diagram of the Drude oscillator model applied to a water dimer.

represented by

$$H_{osc} = -\frac{1}{2m_o}\nabla_o^2 + \frac{1}{2}k\left(X^2 + Y^2 + Z^2\right) \qquad (5)$$

where $\left(X^2 + Y^2 + Z^2\right) = R^2$, R is the distance between the two charges on the oscillator, and m_o is the mass of the oscillator.

Electrostatic interactions include the excess electron interacting with the permanent charges and intermolecular induced dipole moments on the water monomers, but do not include polarization or dispersion effects. The neglect of polarization is one of the major drawbacks to modern force fields. Because atomic charges are selected to give a dipole moment which is larger than the observed value, the average polarization is implicitly included in the parameterization. This means that the effective dipole moment of H_2O is 2.5D in ice and 1.8D in the gas phase.[21] The standard electrostatic energy only contains two-body contributions but when dealing with polar species, 3-body contributions are considered significant. The 3-body effect is considered as the interaction between two charge distributions, which is modified by the presence of a third charge distribution.

To the electrostatic energies and repulsive interactions we add the second-order correction, which is separated into polarization and dispersion interactions between the excess electron and the Drude oscillators. Polarization is proportional to $\frac{q^2}{k}$, which is the polarizability of a Drude oscillator. For our research, polarization values are set equal to the value of a water monomer for a particular water-water model. The second-order dispersion contribution is

$$\varepsilon^{disp} = \sum_s \sum_{\beta \neq 0} \frac{\frac{q^2}{2k}\left|\langle 0|\frac{s}{r^3}|\beta\rangle\right|^2}{-1 + \left(\varepsilon_0 - \varepsilon_\beta\right)\sqrt{\frac{m_0}{k}}} \qquad (6)$$

where the first sum is over *x*, *y* and *z* and the second sum is over the excited states. For the Drude model, we treat the intermolecular induction with Drude oscillators but treat intermolecular dispersion with the Lennard-Jones terms in the water-water model. This method allows us to achieve inclusion of the 3-body induction and dispersion effects for monomers and for electron/monomer interactions.

Lastly, the CI method also includes higher-order correlation effects between the excess electron and the Drude oscillator. In the CI method the trial wave function is written as a linear combination of determinants. The expansion coefficients are determined by requiring that the energy should be a minimum. The CI wave function is

$$\Psi_{CI} = a_0\Phi_{SCF} + \sum_S a_S\Phi_S + \sum_D a_D\Phi_D + \sum_T a_T\Phi_T + ... = \sum_{i=0} a_i\Phi_i \qquad (7)$$

where the sums are over the singly, doubly, triply, etc. excited determinants relative to the HF contribution.

To extend the Drude model to a cluster of molecules, the interactions between the excess electron and each monomer are included in the Hamilitonian. A Drude oscillator is associated with each monomer to treat the polarization and dispersion interactions. The Hamitonian for the excess electron and *j* Drude oscillators is

$$H = H_e + \sum H_j^o + \sum V_j^{e,o} \qquad (8)$$

Where *j* is the number of oscillators, H_j^o is the Hamiltonian for the j^{th} Drude oscillator, and $V_j^{e,o}$ is the coupling between the excess electron and the j^{th} Drude oscillator.

3.2 WATER-WATER MODELS

The water model describes the interactions of water molecules with each other. Early water potentials were composed of "effective" two-body pairwise additive interaction terms. For example, the TIPnP models, popular for biological simulations, treat polarization implicitly by choosing charges that create a large dipole moment.[22] The TIP4P[23] model is an example of this type of potential, where the total energy can be separated into contributions from each atomic pair. While these types of models work well for liquid simulations, they do not give reliable results for clusters. The water-water interactions used in more recent models include electrostatic (charge-charge), charge-induced dipole, and Lennard-Jones type interactions. The induced dipoles on the monomers interact and the polarization equations thus give the net induced dipole moments self-consistently. These recent approaches have resulted in several new interaction potentials, including the Dang-Chang model, which has one polarizable site on each water monomer and the Thole-type Model (TTM), which has three polarizable sites.

3.2.1 Dang-Chang Model

The original Drude code incorporated the DC water model. This model was originally thought to predict accurate neutral water cluster energies.[24] However, further studies show that the model seriously underestimates the energy of the neutral water clusters, thus incorrectly describing the

energies of the anionic clusters. This is due to the fact that the model only has one polarizable site. The DC model is a rigid monomer potential that employs three point charges and one polarizable site. The point charges are: +0.519 on each H atom and -1.038 on the M site, which is located 0.215Å from the O atom in the direction of the H atoms. A 6-12 Lennard-Jones site is associated with the O atom of each monomer and an isotropic polarizable site with the same polarizability as the experimental value, 1.444Å^3, is located at the M site.

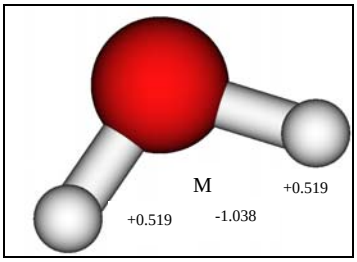

Figure 3.2.1 Dang-Chang model charges applied to a water monomer.

In order to use the DC model to describe excess electron interactions, Feng Wang, a former group member, replaced the single polarizable site with a Drude oscillator with the same polarizability. While the DC model is an improvement over earlier models, such as the TIP-nP models, it does not accurately reproduce the relative energies of various isomers of neutral water clusters obtained by MP2 calculations. This inaccuracy is due to the failure to accurately calculate the polarization, due to the limitations of the use of a single polarizable site. For this reason, we have considered the TTM2-R water model of Xantheas *et al.*[25]

3.2.2 Thole-type Model

In 1999, Xantheas *et al.*[6] reported a model for describing water clusters based on the Thole[26] method of using smeared charges and dipoles. The TTM model employs three atom-centered polarizable sites (one on O and two on H) with Thole-type damping. Thole determined the smearing function width and polarizabilities of H,

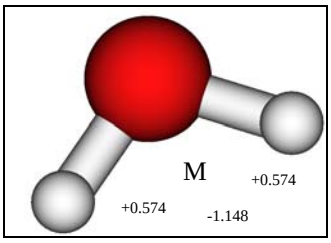

Figure 3.2.2 Charges used in the TTM model.

C, N and O in order to closely reproduce the molecular polarizabilities for a variety of molecules. Xantheas *et al.* demonstrated that the TTM potential gives binding energies that are in good agreement with *ab initio* results for water clusters.

The TTM2-R model uses the same Thole smearing charges as in the TTM model, but offers a reparameterization of the two-body part of the potential, based on *ab initio* calculations. In spite of the success of the TTM2-R model, Defusco, in the Jordan group, has shown that it is underpolarized, based on 3-body calculations. To fix this problem, DeFusco changed the charge-dipole damping factor from 0.2 to 0.3. Several other changes were also made, and the resulting water model is designated Distributed Point Polarization, or DPP.

DeFusco and Sommerfeld from our group have combined the DPP water model with the Drude approach for describing excess electrons in clusters. I have used this approach in my study of $(H_2O)_6^-$. In the next section, I discuss the methodology of parallel tempering Monte Carlo (PTMC) simulations.

3.3 PARALLEL TEMPERING MONTE CARLO METHODS

Our work utilized a PTMC method for the finite temperature simulations. Parallel tempering refers to running simulations at several temperatures in parallel, each on a different processor. Metropolis[27] Monte Carlo simulations are used to explore a potential and aid in determining a low-energy geometry. Monte Carlo simulations involve randomly moving one or more atoms of a system to give a new configuration. The new geometry is accepted if the new configuration is lower in energy than the previous configuration. If the new configuration is higher in energy, a

random number between 0 and 1 is generated and the Boltzmann factor calculated as

$$B = e^{-E_{new} - E_{old} / k_B T} \qquad (9)$$

where k_B is the Boltzmann constant and T is the temperature in Kelvin.

If the result is less than the random number, the new configuration is accepted. Otherwise, the previous configuration is retained and the procedure is repeated.[28] During the PTMC process, pairs of temperatures are occasionally exchanged (*Figure 3.3).* This method is useful because the temperature exchanges make it easier for the cluster to escape local minima. For our work, the temperatures were exchanged after every 250 Monte Carlo moves. In addition, PTMC does not require storage of the configurations because the exchanges are not predetermined.[29] The PTMC method can be combined with simulated annealing to find the global minimum of a system.

For our work, we used several sets of eight temperatures, run in parallel. The final set of temperatures ranged from 30-120K. To overcome energy barriers, adjacent temperatures were exchanged after a predetermined number of moves. We ran our simulations in sets of one million moves and each successive set was started from the previous set's final geometry. The maximum step size was chosen so that 50% of the moves were accepted.

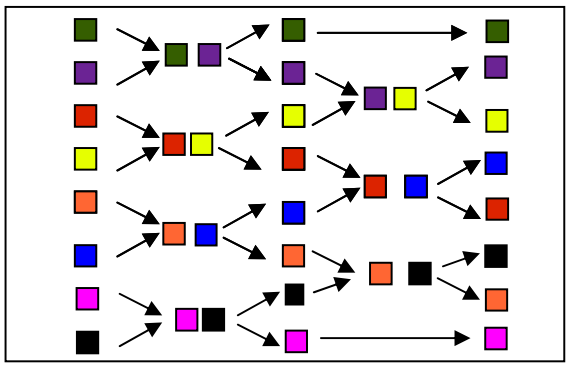

Figure 3.3 Schematic diagram of parallel-tempering temperature changes.

4.0 APPLICATIONS

4.1 DRUDE/DC APPROXIMATION STUDY

In coding the Drude/DC model, Wang incorporated an approximation into the code to speed up the simulations. This approximation did not use the Drude model to recalculate the electronic energy if the change in the dipole moment was small (less than 2%); instead, the EBE from the previous step was added to the new energy of the neutral water cluster to obtain an approximate energy for the anion. In my work I simulated $(H_2O)_6^-$ using the PTMC method and the Drude/DC model both with and without the above approximation. *Figures 4.1.1* and *4.1.2* show the results of these PTMC simulations. *Figure 4.1.1* shows that the approximation results in a dominant isomer with an EBE near 0.1 eV. However, the DC model actually predicts a dominant isomer of OP-AA, with an EBE near 0.5 eV. These results show that, although the approximation does not affect the total energy of the structures, it does introduce a sampling bias. *Figure 4.1.2* illustrates the results of the Drude/DC model without the approximation. From this figure we can see that the sampling is no longer biased towards a particular structure but instead the expected OP2-AA isomer is dominant.

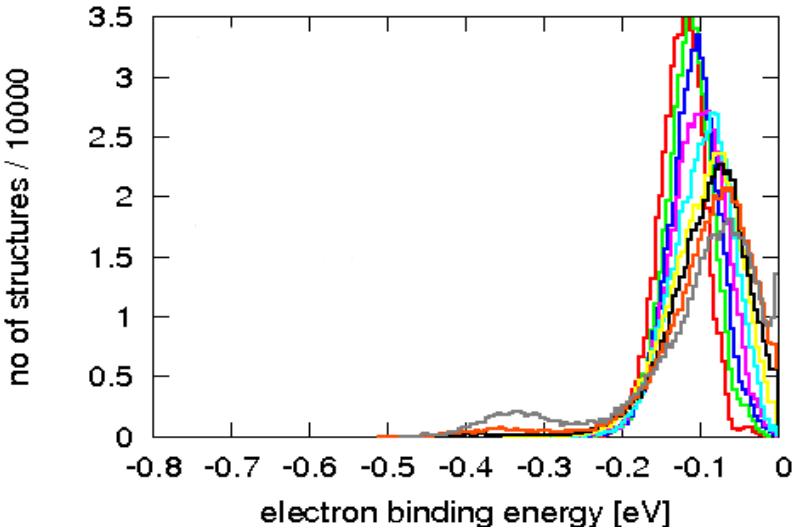

Figure 4.1.1 Electron binding energy distributions from PTMC Dang-Chang/Drude model simulations with the fast simulation mode.

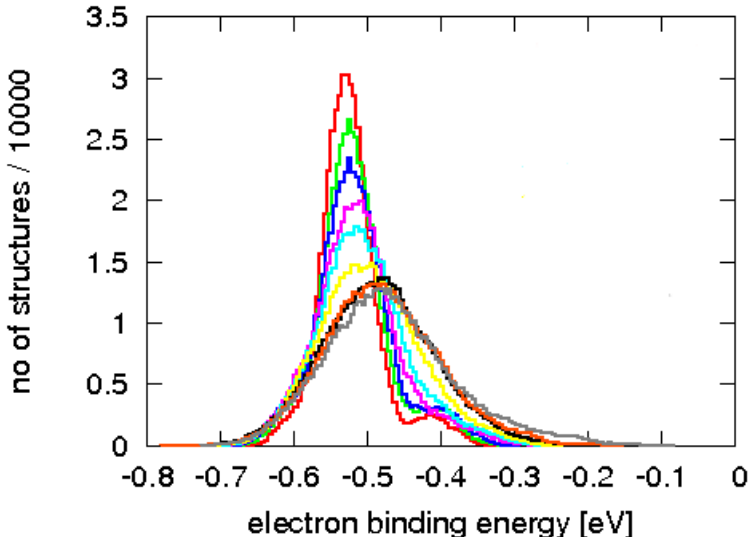

Figure 4.1.2 Electron binding energy distributions from PTMC Dang-Chang/Drude model simulations without the fast simulation mode.

4.2 FINITE TEMPERATURE SIMULATIONS WITH THE DPP MODEL

These PTMC simulations were carried out for T = 50 -179K, geometrically-scaled. Seven million Monte Carlo moves were made. The simulations were found to have frequent auto-detachment events, caused by the high simulation temperatures. A lower temperature range, T= 30-120K, was adopted with the Drude/DPP model potential to minimize this problem and to obtain EBE distributions that reflected the expected isomers at the appropriate binding energies. This set of temperatures was 30, 37, 45, 54, 66, 81, 99, and 121K.

To ensure that equilibrium was reached, two separate isomers, Cage 1 (CA1) and OP2-AA, were used to start the PTMC simulations. A total of eight million Monte Carlo moves were made and the last four million moves were kept as production runs in each case. The production runs starting from the two structures gave nearly identical results, which reassures us that the simulations have achieved equilibrium. *Figures 4.2.1- 4.2.4* show the results of the first and fifth million Monte Carlo moves. It is clear that, initially, the sampling is not at equilibrium because both starting structures (*Figure 4.2.1 and 4.2.3)* are the dominant isomer at their respective EBEs. However, by the time the fifth million set of moves is complete, the sampling has equilibrated and the two different starting isomers converge to the same dominant isomer in the end. In this case, it is the CA1 isomer.

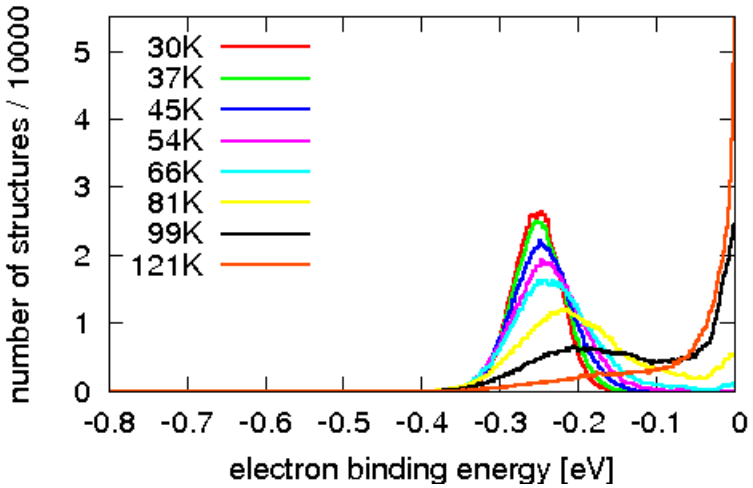

Figures 4.2.1 EBE distributions of the first million Monte Carlo moves started from equilibrium and started from the CA1 isomer. The first million moves were thrown out as equilibrium data.

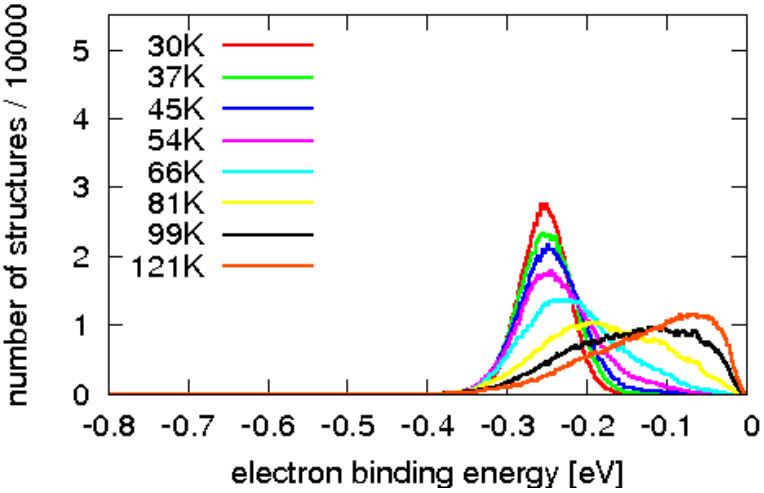

Figures 4.2.2 EBE distributions of the fifth million Monte Carlo moves started from the resulting configurations of the fourth million Monte Carlo moves (CA1).

.

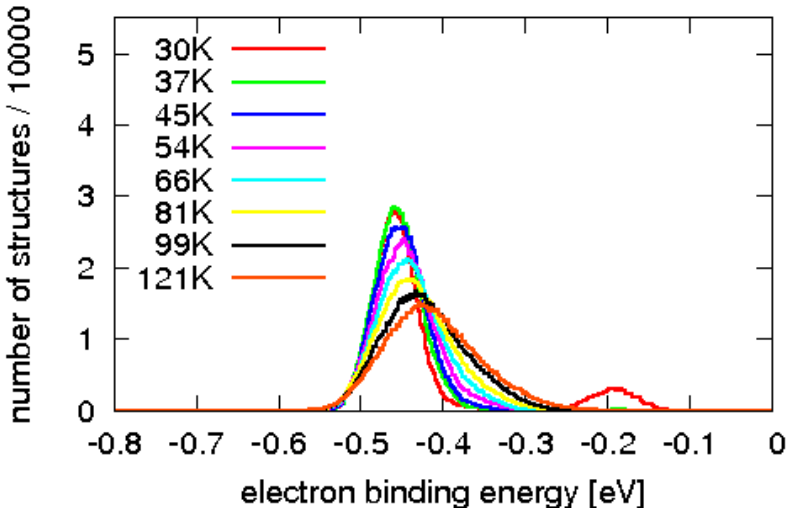

Figures 4.2.3 EBE distributions of the first million Monte Carlo moves started from equilibrium and started from the OP2-AA isomer. The first million moves were thrown out as equilibrium data.

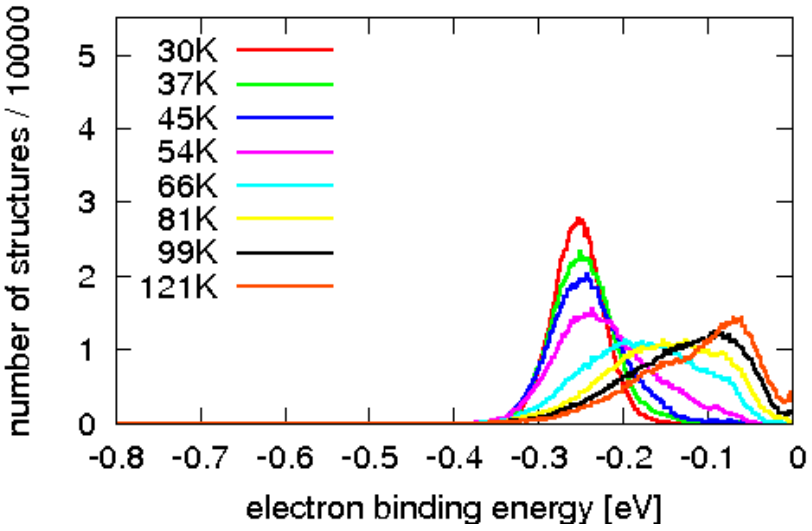

Figures 4.2.4 EBE distributions of the fifth million Monte Carlo moves started from the resulting configurations of the fourth million Monte Carlo moves (OP2-AA).

After the parallel tempering simulations were completed, several thousand structures were quenched to determine their inherent structures. Over 15 isomers were identified within 60 meV (1.5 kcal/mol) of the global minimum (*Figure 4.2.5)*. At T=54K, the dominant isomers are those with EBEs lower than that of OP1-AA and OP2-AA isomers, which are the isomers found with the Drude/DC model. The dominant isomers are the CA1 and OP1.

The results of the finite temperature simulations were that the Drude/DPP model potential gave a dominant isomer with an EBE near 0.25 eV, while the Drude/DC model, as shown in the fast simulation mode study, gave a dominant isomer with an EBE near 0.5 eV.

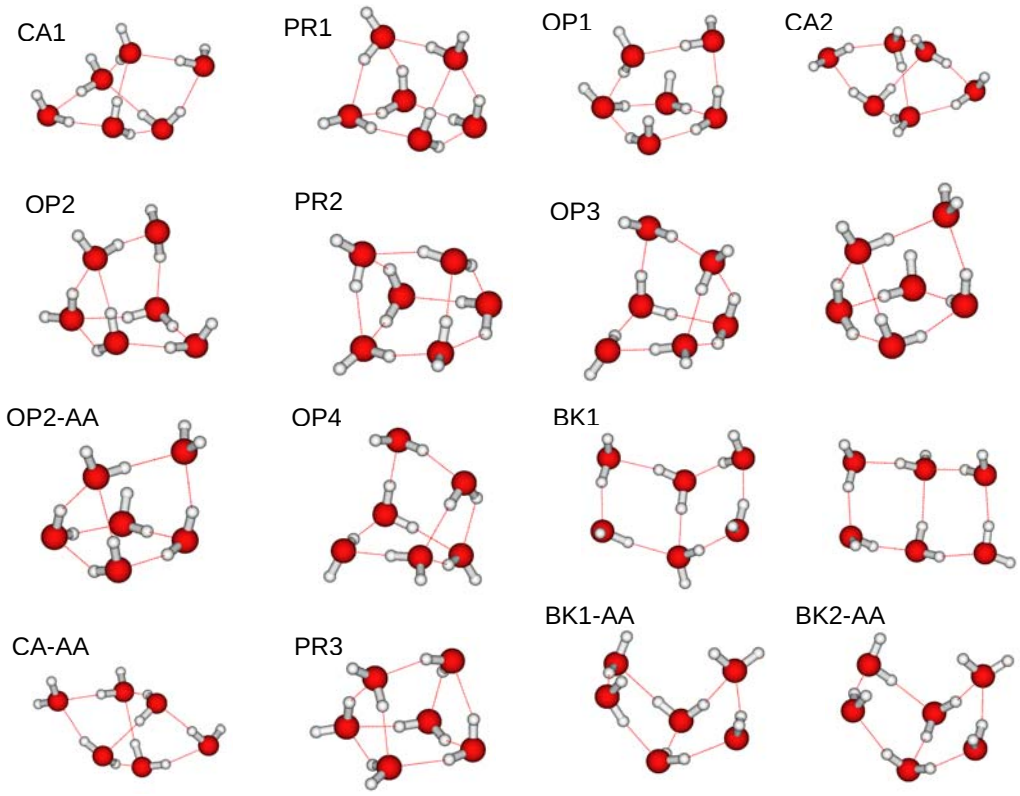

Figure 4.2.5 $(H_2O)_6^-$ low-energy isomers

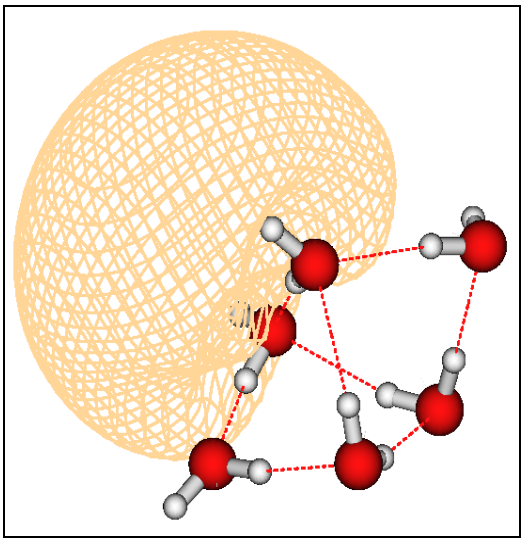

Figure 4.2.6 Charge density distribution of CA1 isomer.

4.3 LOW-ENERGY ISOMER STUDY

After the PTMC simulations were complete, several low-energy isomers were re-optimized at the *ab initio* MP2 level of theory using two different basis sets. The first basis set was taken from Herbert and Head-Gordon. It consists of the 6-31++G* basis set[30] with two diffuse s-type functions on the H atoms. The exponents for these diffuse functions are 0.012 and 0.004. The second basis set is the aug-cc-pVDZ basis set[31] plus a 4s3p set of diffuse functions on a single O atom. The exponents for the second basis set range from 0.015 to 0.00012 for the s-type functions and 0.012 to 0.00048 for the p-type functions. The *ab initio* calculations were carried out with the Gaussian03[32] computer program.

Ab initio MP2 calculations were performed on the five low-energy isomers that were found with the DPP PTMC simulations. Those isomers were: CA1, CA-AA, OP1, OP2-AA, and BK1-AA. The OP2-AA is the experimentally-observed dominant isomer, which has been

predicted in prior theoretical students as being the most stable isomer of $(H_2O)_6^-$.[33,34,35,36]

The relative energies from the Drude/DPP model calculations are in reasonable agreement with the results of the MP2 calculations with the larger basis set results (*Figure 4.3.1).* Application of high-order corrections to the large basis set MP2 energies brings the relative energies from the *ab initio* and Drude/DPP model calculations even closer.

The MP2 calculations predict the CA1 isomer to be the most stable isomer of $(H_2O)_6^-$. The experimentally-observed OP2-AA isomer is predicted to be significantly higher in energy than the global minimum isomer. Our results provide clear evidence that the experimentally-found OP2-AA isomer is not the most stable form of $(H_2O)_6^-$ (*Figure 4.3.2).*

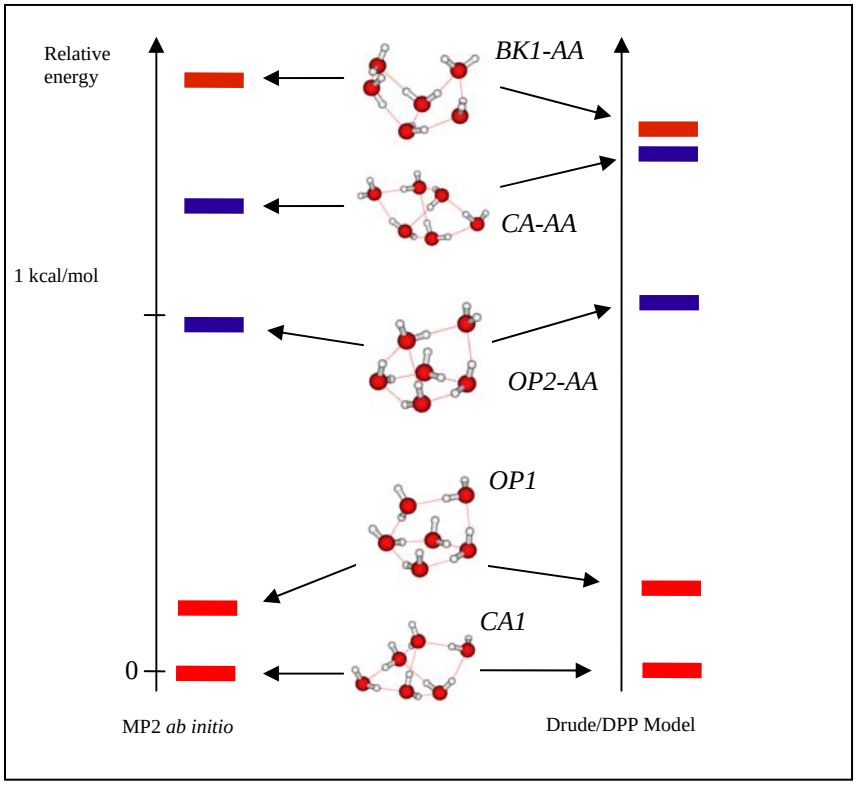

Figure 4.3.1 Relative energies of various isomers of $(H_2O)_6^-$ as described by the Drude/DPP model and by MP2 calculations. These MP2 results employed the Herbert basis set.

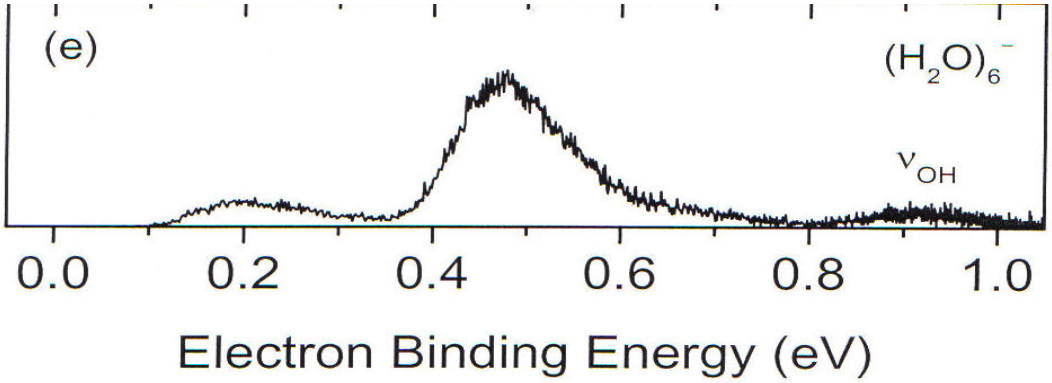

Figure 4.3.2 Experimental photoelectron spectrum of $(H_2O)_6^-$ (N. Hammer, J. Roscioli, J. Bopp, J. Headrick, M. Johnson,

To determine the inadequacies of the Drude/DC model, we have to look at the polarization and repulsive interactions. The DC water-water model does not have repulsive interactions between the H atoms on the water monomers, which creates a bias towards prism-like structures, where several nearby OH groups point towards the excess electron. The polarization is also underestimated in the Drude/DC model, and this introduces errors in the relative energies of the isomers. This leads us to conclude that it is essential that the water model correctly describes the neutral water clusters at the geometries which they assume as anions.

Table 4.3. Relative energies, dipole moments, and electron binding energies of low-energy isomers, from the DPP model.

Isomers	***Relative Energy (meV)***	***Dipole Moment (Debye)***	***Electron Binding Energy (meV)***
CA1	0	6.9	197
PR1	2	6.4	146
OP1	3	6.5	141
CA2	13	6.9	203
OP2	22	5.5	102
PR2	22	6.2	141
OP3	23	5.4	78
OP1-AA	45	9.4	432
OP2-AA	48	9.5	440
OP4	54	4.2	29
BK1	56	4.8	92
BK2	64	3.7	23
CA-AA	72	8.6	338
PR3	74	9.4	382
BK1-AA	80	8.6	430
BK2-AA	83	8.9	442

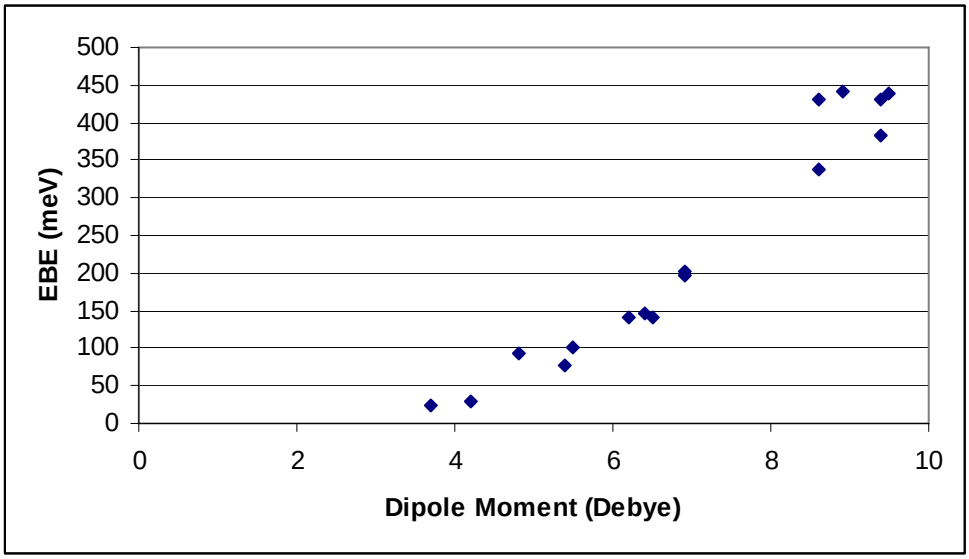

Figure 4.3.3 Dipole moment correlation to electron binding energy

5.0 CONCLUSIONS

From our simulations, we have determined that the approximation made by Wang and Jordan to speed up the Monte Carlo simulations introduces a bias into the population sampling. Therefore, the fast simulation should not be used for PTMC simulations. Our calculations also revealed that to correctly describe the relative energies of various isomers it is essential to employ a water model with polarizable sites and repulsive interactions involving H atoms. Our finite temperature simulations show that the anion population is dominated by clusters with EBEs less than 200 meV. Our calculations show that several isomers exist at lower energies than the AA species and the OP2-AA isomer observed experimentally accounts for a small percent of the isomers found with the PTMC simulations and quenching. From this observation, we conclude that the experimentally-found clusters are not sampled at equilibrium.

6.0 FUTURE WORK

The methods used in this study are applicable to other systems. One important extension would be to the $(NH_3)_n^-$ clusters. Bowen has seen anionic ammonia clusters with n > 40 experimentally, but has not seen smaller clusters.[37] Another cluster that would be interesting to model is $(CO_2)_n^-$. Unlike the water and ammonia molecules, the undistorted carbon dioxide molecule does not have a dipole moment. Moreover, upon bending, the anion acquires some valence character, making the $(CO_2)^-$ clusters an interesting test case for the Drude model. Another important extension is to incorporate into the force field the ability of the water molecules to undergo stretching and bending motions. This capability is essential for the calculation of the vibrational spectrum.

REFERENCES

[1] Garrett, *et al*, Chem. Rev. **105**, 355 (2005).
[2] J. R. R. Verlet and A. Kammrath, G. B. Griffin, and D. M. Neumark, J. Chem. Phys. **123**, 231102 (2005).
[3] L. Turi, W. Sheu, and P. Rossky, Science **309**, 914 (2005).
[4] J. R. R. Verlet, A. E. Bragg, A. Kammrath, O. Cheshnovsky, and D. M. Neumark, Science **307**, 93 (2005).
[5] N. I. Hammer, J. R. Roscioli, and M. A. Johnson, J. Phys. Chem. A. **109**, 7896 (2005).
[6] C. J. Burnham, J. Li, S. S. Xantheas, and M. Leslie, J. Chem. Phys. **110**, 4566 (1999).
[7] T. Sommerfeld and K. D. Jordan, J. Phys. Chem. A **109**, 11531 (2005).
[8] F. Wang and K. D. Jordan, J. Chem. Phys. **119**, 11645 (2003).
[9] F. Wang and K. D. Jordan, J. Chem. Phys. **116**, 6973 (2002).
[10] J.-W. Shen, N. I. Hammer, J. M. Headrick, and M. A. Johnson, Chem. Phys. Lett., **399**, 3419 (2004).
[11] S. K. Blau, Physics Today, **58**, 21 (2005).
[12] T. Sommerfeld and K. D. Jordan (unpublished).
[13] E. Myshakin, K. Diri, andn K. D. Jordan, J. Phys. Chem. A, **108**, 6758 (2004).
[14] N. I. Hammer, J.-W. Shin, J. M. Headrick, E. G. Diken, J. R. Roscioli, G. H. Weddle, and M. A. Johnson, Science **306**, 675 (2004).
[15] J. Herbert and M. Head-Gordon, J. Phys. Chem. A. **109**, 5217 (2005).
[16] J. M. Herbert and M. J. Head-Gordon, Phys. Chem. Chem. Phys. **8**, 68 (2006).
[17] M. Rigby, E. B. Smith, W. A. Wakeham, and G. C. Maitland, *The Forces Between Molecules* (Clarendon, Oxford, 1986).
[18] L. X. Dang and T. M. Chang, J. Chem. Phys. **106**, 8149 (1997).
[19] J. Schniker and P. J. Rossky, J. Chem. Phys. **86**, 3462 (1987).
[20] F. Wang and K. D. Jordan, J. Chem. Phys. **114** 10717 (2001).
[21] F. Jensen, *Introduction to Computational Chemistry*(John Wiley and Sons, Inc, New York, 1999).
[22] A. DeFusco, Comprehensive Exam Document, University of Pittsburgh, November 21, 2005
[23] W. L. Jorgenson, J.Chandrasekhar, J. D. Madura, R. W. Imprey, and M. L. Klein, J. Chem. Phys. **79**, 926 (1983).
[24] J. M. Pedulla and K. D. Jordan, Chem. Phys. **239**, 593 (1998).
[25] C. J. Burnham and S. S. Xantheas, J. Chem. Phys. **116**, 1500 (2002).
[26] B. T. Thole, Chem. Phys. **59**, 341 (1981).
[27] N. Metropolis, A. W. Rosenbluth, M. N. Rosenbluth, A. H. Teller, and E. Teller, J. Chem. Phys. **21**, 1087 (1953).
[28] A. Leach, "Molecular Modelling: Principles and Applications," Essex: Addison Wesley Longman Ltd, 1996.
[29] A. N. Tharrington and K. D. Jordan, J. Phys. Chem. **107**, 7380 (2003).
[30] W. J. Hehre, R. Ditchfield, and J. A. Pople, J. Chem. Phys. **56**, 2257 (1972).
[31] R. A. Kendall, T. H. Dunning, Jr., and R. J. Harrison, J. Chem. Phys. **96**, 6769 (1992).
[32] GAUSSIAN, computer code Gaussian03, Revision B. 03, 2003.
[33] F. Weigend and R. Ahlrichs, Phys. Chem. Chem. Phys. **1**, 4537 (1999).
[34] S. B. Suh, H. M. Lee, J. Kim, J. Y. Lee, and K. S. Kim, J. Chem. Phys. **113**, 5273 (2000).
[35] H. M. Lee, S. B. Suh, and K. S. Kim, J. Chem. Phys. **119**, 7685 (2003).
[36] H. M. Lee, S. B. Suh, P. Tarakeshwar, and K. S. Kim, J. Chem. Phys. **122**, 44309 (2005).
[37] H. W. Sarkas, S. T. Arnold, J. G. Eaton, G. H. Lee, and K. H. Bowen, J. Chem. Phys. **116**, 5731 (2002).